Experimental Neurology 314 (2019) 100–110

Contents lists available at ScienceDirect

Experimental Neurology

journal homepage: www.elsevier.com/locate/yexnr

Research paper

Long non-coding RNA AK038897 aggravates cerebral ischemia/reperfusion injury *via* acting as a ceRNA for miR-26a-5p to target DAPK1

Rui Wei[a], Lin Zhang[b], Wei Hu[a], Jie Wu[a], Wei Zhang[a,*]

[a] Department of Emergency Medicine, The First Affiliated Hospital of Kunming Medical University, No. 295 Xichang Road, Wu Hua District, Kunming 650032, Yunnan Province, China

[b] Department of Rehabilitation M edicine, The First Affiliated Hospital of Kunming Medical University, No. 295 Xichang Road, Wu Hua District, Kunming 650032, Yunnan Province, China

ARTICLE INFO

Keywords:
LncRNA
AK038897
Ischemic stroke
MiR-26a-5p
Death-associated protein kinase 1
Apoptosis

ABSTRACT

Emerging evidence has suggested a significant role of long non-coding RNAs (lncRNAs) in ischemic stroke by acting as competing endogenous RNAs (ceRNAs) for microRNAs (miRNAs) to regulate certain RNA transcripts. AK038897 is an lncRNA that was reported to be upregulated in rat brains in response to transient focal ischemia. We aimed to investigate the possible regulatory role of AK038897 in ischemic stroke. We detected increased AK038897 and decreased miR-26a-5p levels in mouse brains following middle cerebral artery occlusion/reperfusion (MCAO/R) and in neuro-2A (N2a) neuroblastoma cells following oxygen–glucose deprivation and reoxygenation (OGD/R). With bioinformatics, we identified shared putative miR-26a-5p binding sites in AK038897 as well as in the 3′-UTR of death-associated protein kinase 1 (DAPK1), which is a central mediator of ischemic neuronal death. MiR-26a-5p overexpression attenuated OGD/R-induced N2a cell apoptosis. The luciferase reporter assay results confirmed that miR-26a-5p directly targets DAPK1. Further studies showed that AK038897 directly binds to miR-26a-5p and functions as a ceRNA for miR-26a-5p to regulate DAPK1. As a result, AK038897 overexpression antagonized while AK038897 knockdown enhanced the inhibitory effects of miR-26a-5p on DAPK1 expression and OGD/R-induced N2a cell apoptosis. Further, AK038897 knockdown protected against MCAO/R-induced brain injury and neurological deficits *in vivo*. In summary, we identified a AK038897/miR-26a-5p/DAPK1 signaling cascade as a key mechanism controlling cerebral ischemia/reperfusion injury. Pharmaceutical intervention of this cascade may provide novel therapy for ischemic insults.

1. Introduction

Stroke is the second most frequent cause of mortality after coronary artery disease, accounting for 6.3 million global deaths in 2015 (Wang et al., 2016). Most reported strokes (approximately 85%) are ischemic strokes, which occur when an embolus or thrombus blocks the blood supply to part of the brain, resulting in brain cell death (Musuka et al., 2015). Currently, the only clinically effective therapy for acute ischemic stroke is intravenous administration of recombinant tissue plasminogen activator (tPA) to rapidly restore cerebral blood flow (Blakeley and Llinas, 2007). Although timely reperfusion can minimize brain cell damage, restoration of blood supply after a period of ischemia frequently results in ischemia/reperfusion (I/R) injury of brain cells and consequent exacerbation of brain tissue damage. This secondary brain injury progresses rapidly in the first few days following cerebral ischemia, and then at a slower rate for up to 2 weeks (Nour et al., 2013). Thus, understanding the mechanisms governing cerebral I/R injury is essential for the discovery of new strategies to control ischemic stroke-associated brain damage.

Non-coding RNAs (ncRNAs) are functional RNA molecules that are not translated into proteins but can regulate the expression and function of many protein-coding genes. Studies have shown that cerebral ischemia profoundly impacts the expression profiles of various ncRNA species such as microRNAs (miRNAs, 20–25 nt) and long non-coding RNAs (lncRNAs, > 200 nt) (Dharap et al., 2009; Dharap et al., 2012). A large body of evidence has demonstrated miRNAs as critical mediators of posttranscriptional gene silencing in pathogenic mechanisms of ischemic stroke, such as excitotoxicity, inflammation, neuronal apoptosis and neurogenesis (Li et al., 2018). As a result, a subset of miRNAs are being actively pursued as neurorestorative therapy for ischemic stroke (Martinez and Peplow, 2017). Compared with that of miRNAs, the function of lncRNAs in stroke pathogenesis is much less well

* Corresponding author at: Department of Emergency Medicine, The First Affiliated Hospital of Kunming Medical University, No. 295 Xichang Road, Wu Hua District, Kunming 650032, Yunnan Province, China.
E-mail address: zhangwei7222@126.com (W. Zhang).

https://doi.org/10.1016/j.expneurol.2019.01.009
Received 29 August 2018; Received in revised form 18 December 2018; Accepted 12 January 2019
Available online 29 January 2019
0014-4886/

understood. However, emerging evidence has suggested a functional engagement of lncRNAs in ischemic stroke by acting as competing endogenous RNAs (ceRNAs) that regulate specific RNA transcripts through competing for shared miRNAs (Guo et al., 2017; Yan et al., 2017). This lncRNA–miRNA crosstalk might be a prominent mechanism controlling cerebral I/R injury and post-ischemia recovery.

AK038897 is an lncRNA that was found to be drastically upregulated in rat brains subjected to transient focal ischemia (Wu et al., 2017); however, the function of AK038897 in ischemic stroke is not defined. In this work, we investigated the regulatory function of AK038897 in oxygen-glucose-deprivation/reoxygenation (OGD/R)-stimulated neuronal death *in vitro* and in middle cerebral artery occlusion/reperfusion (MCAO/R)-induced brain damage *in vivo*. We found AK038897 was physically associated with miR-26a, the most suitable candidate for further analysis. By contrast, miR-6876-5p, miR-383-3p, miR-9-5p, miR-517-5p, miR-145-5p, miR-15a-5p, miR-107, miR-103a-3p and miR-449a-3p, although they possess putative binding sites in AK038897 with bioinformatics, they did not display any correlation at expression levels (Supplementary materials). Increasing evidences show that miR-26a has an important role in mediating cells proliferation and apoptosis processes. Feng et al. found that miR-26a level was decreased, and overexpressing miR-26a inhibited the pathogenesis in a mice model of atherosclerosis, a chronic inflammatory disease and a major cause of life-threatening complications, such as myocardial infarction and stroke (Feng et al., 2018). MiR-26a-5p was also reported to inhibited endothelial apoptosis by suppressing TLR4/NF-κB pathway in human endothelial cells (Zhong et al., 2018). In addition, AK038897 competed with DAPK1 (Death-associated protein kinase 1) mRNA containing an offset 8-mer seed site for binding to miR-26a and contradicted the inhibitory effects of miR-26a on DAPK1 to regulate ischemic neuronal death. DAPK1 is a death domain-containing serine/threonine kinase that is regulated by calcium/calmodulin (Bialik and Kimchi, 2006), which was first identified in 1995 as a mediator of interferon-γ-induced apoptosis (Deiss et al., 1995). Later studies have revealed its involvement in multiple apoptotic pathways induced by various stimuli such as Fas, TNF-α and ceramide (Cohen et al., 1999; Pelled et al., 2002). In particular, DAPK1 is activated in response to cerebral I/R and functions as a central mediator of ischemic neuronal death *in vitro* and *in vivo* (Shamloo et al., 2005; Tu et al., 2010). Here, we identified a AK038897/miR-26a-5p/DAPK1 axis that controls neuronal I/R injury *in vitro* and *in vivo*, which may inform novel therapeutic strategies for ischemic stroke.

2. Materials and methods

2.1. Mouse model of focal cerebral I/R

Although rat models have been used to promote the development in many fields of medical research, lots of genetic techniques widely used in mice are not possible in rats at the present. The mice model is more suitable for gene function analysis, so we performed the remaining work in mice and in the cell line from mice. Male C57BL/6J mice (8–10 weeks of age) were purchased from the Experimental Animals Center at Kunming Medical University (Kunming, Yunnan, China). Focal cerebral ischemia was established by intraluminal MCAO following previously reported procedures (Yan et al., 2016). Reperfusion was established 1 h later. The animals were anesthetized with pentobarbital sodium (30 mg/kg) and placed on a heating panel maintained at 37.0 °C ± 0.5 °C during the entire operation. Regional ischemia (a drop in blood flow as 80% relative to baseline) and reperfusion (blood flow > 70% of baseline) were confirmed by laser Doppler flowmetry (Moor Instruments, Oxford, UK). After 24 h of reperfusion, the animals were sacrificed by decapitation. Sham-operated mice underwent the same surgical procedure except MCAO. All animal studies were conducted in compliance with the American Animal Protection Legislation and with ethical approval by the Institutional Animal Care and Use Committee of the First Affiliated Hospital of Kunming Medical University.

2.2. Cell culture and OGD/R model

Mouse Neuro-2A (N2a) neuroblastoma cells were obtained from the Cell Bank of Shanghai Institute of Cell Biology, Chinese Academy of Sciences (Shanghai, China). The cells were maintained in Dulbecco's Modified Eagle's Medium (DMEM; Invitrogen) supplemented with 10% fetal bovine serum (FBS; Invitrogen), 2 mM glutamine (Invitrogen), 100 μg/ml streptomycin (Invitrogen) and 100 U/ml penicillin (Invitrogen) at 37 °C, 5% CO_2 in a humidified incubator. For OGD treatment, the cells were placed in deoxygenated glucose-free Hanks' Balanced Salt Solution (Invitrogen) and incubated in a hypoxic chamber containing 5% CO_2 and 95% N_2 at 37 °C for 3 h. After that, the cells were transferred to normal culture medium and maintained under normoxic conditions (5% CO_2) at 37 °C for 24 h.

2.3. RNA extraction and quantitative real-time PCR (qRT-PCR)

Total RNA and miRNAs were extracted using Trizol reagent (Invitrogen) and miRNeasy Mini Kit (Qiagen), respectively. For miRNA analysis, cDNA was obtained using the TaqMan MicroRNA Reverse Transcription Kit (Applied Biosystems, Foster City, CA, USA). The expression of miR-26a-5p was quantified by RT-PCR using the TaqMan miRNA assay kit (Applied Biosystems). Data were normalized to U6 small nuclear RNA (U6 snRNA). For mRNA analysis, cDNA was synthesized using M-MLV reverse transcriptase (Invitrogen) and Oligo(dT) reverse transcription primers. The expression of AK038897 and DAPK1 was quantified by PCR using SYBR Green Real-Time PCR Master Mixes (ThermoFisher, Waltham, MA, USA). Data were normalized to GAPDH. All amplification assays were performed on a 7900HT Fast RealTime PCR machine (Applied Biosystems). Primer sequences used in PCR are as follows: AK038897, 5′-GCTGTAGCATCCTAGCGGTT-3′ (forward) and 5′-TCAAAGGAAGAAGAAACATCCTGT-3′ (reverse); DAPK1, 5′-CCGAGACCTGAGTAGTGGGA-3′ (forward) and 5′-GTGCTTCACCGT CAACAACC-3′ (reverse); GAPDH, 5′-TGTGAACGGATTTGGCCGTA-3′ (forward) and 5′-GGTCTCGCTCCTGGAAGATG-3′ (reverse); miR-26a-5p, 5′-GTCGTATCCAGTGCAGGGTCCGAGGTATTCGCACTGGATACGA CTGTTAAGA-3′ (loop), 5′-TGCGCAACATCACTGCAAGTCT-3′ (forward) and 5′-CCAGTGCAGGGTCCGAGGTATT-3′ (reverse); U6, 5′-CGCTTCG GCAGCACATATAC-3′ (forward) and 5′-AAATATGGAACGCTTCA CGA-3′ (reverse).

2.4. Western blot analysis

Total protein was extracted from cells and cerebral tissues using RIPA lysis buffer containing protease inhibitors. Samples (30 μg) were separated by gel electrophoresis on 10% sodium dodecyl sulfate polyacrylamide gels (SDS-PAGE) and subsequently transferred to PVDF membranes (Millipore, Bedford, MA, USA). After blocking in 5% nonfat milk for 2 h, the membranes were incubated overnight at 4 °C with primary antibodies toward DAPK1 (Abcam, Cambridge, MA, USA), cleaved caspase-3 (C-caspase-3) (Abcam), cleaved PARP (C-PARP) (Cell Signaling Technology, Boston, USA), Bcl-2 (Santa Cruz Biotechnology, Santa Cruz, CA, USA), Bax (Santa Cruz Biotechnology) and β-actin (Abcam), respectively. After washing in Tris-buffered saline containing 0.1% Tween 20 (TBST), the membranes were incubated with horseradish peroxidase-conjugated secondary antibody (Santa Cruz Biotechnology) for 1 h at room temperature. The protein bands were visualized with enhanced chemiluminescence (ECL) reagents.

2.5. Luciferase reporter assay

Putative miR-26a-5p binding sites in AK038897 and the 3′-UTR of DAPK1 were predicted using StarBase (http://starbase.sysu.edu.cn/

mirMrna.php) and TargetScan (http://www.targetscan.org), respectively. A wild-type (WT) and mutant (MUT) AK038897 sequence and a WT and MUT 3′-UTR fragment of DAPK1 containing the putative miR-26a-5p binding site were synthesized at Genechem (Shanghai, China) by site-directed mutagenesis using the QuickChange Lightning kit (Stratagene, La Jolla, CA, USA). The mutations were confirmed by sequencing. The constructs were cloned into the pmirGLO dual luciferase reporter vector (Promega, Madison, WI, USA) downstream of the luciferase reporter gene to generate AK038897-WT, AK038897-MUT, DAPK1-WT and DAPK1-MUT luciferase reporter systems. N2a cells were seeded in 24-well plates and transfected with the luciferase reporter plasmids, miR-26a-5p mimic, mimic-NC (nonspecific control for miR-26a-5p mimic), miR-26a-5p inhibitor and inhibitor-NC (nonspecific control for miR-26a-5p inhibitor), alone or in combination for 48 h. Luciferase activity was determined using the Dual-luciferase reporter assay system (Promega, Madison, WI, USA). Relative luciferase activity was normalized to the Renilla luciferase internal control.

2.6. RNA immunoprecipitation assay

N2a cells ($\sim 1 \times 10^7$) transfected with miR-26a-5p mimic or mimic-NC for 48 h were washed with cold PBS and lysed with RNA immunoprecipitation (RIP) lysis buffer (EMD Millipore, Billerica, MA, USA). The cell lysates were incubated with magnetic beads conjugated with anti-Argonaute2 (AGO2) antibody (Millipore) or negative control mouse IgG (Millipore). The beads were collected and washed, and RNAs were extracted in the presence of proteinase K. AK038897 was detected by RT-PCR and qRT-PCR. The cell lysate served as the input.

2.7. Plasmids construction and cell transfection

For AK038897 overexpression, the mouse full-length AK038897 cDNA was subcloned into the pcDNA3.1(+) mammalian expression vector (Invitrogen) at the *Kpn*I and *Xho*I sites to generate pcDNA3.1-AK038897 plasmids. All plasmids were isolated using the DNA Midiprep kit (Qiagen, Germany). N2a cells transfected with pcDNA3.1-AK038897 were selected using G418 (geneticin) to generate stable clones. Cells transfected with the empty pcDNA3.1(+) vector (pcDNA3.1-NC) were used as negative control. For AK038897 knockdown, si-AK038897 (5′-CCTAGCGGTTGGACTCAAA-3′) and si-NC (5′-CCTGGCGTTCAGCTAGAAA-3′, negative control) were prepared at Genechem. For miR-26a-5p overexpression and knockdown, miR-26a-5p mimic, miR-26a-5p inhibitor, as well as two scrambled miRNAs as their corresponding negative controls (mimic-NC for miR-26a-5p mimic and inhibitor-NC for miR-26a-5p inhibitor, respectively) were synthesized at Genechem. All transfections were performed using Lipofectamine 2000 reagent (Invitrogen) following manufacturer's instructions.

2.8. Stereotaxic injection

The animals were anesthetized and fixed to a stereotaxic apparatus (David Kopf Instruments, Tujunga, CA, USA). A total of 5 μl lentivirus si-AK038897 or si-NC (10^9 infectious units/ml; GenePharma, Shanghai, China) was mixed with *in vivo* RNAiMAX transfection reagent (Invitrogen) and administered into the lateral ventricle of mice 24 h before MCAO. The stereotaxic coordinates used were 0.2 mm posterior to bregma, 1.0 mm lateral to the midline and 1.5 mm below the brain surface.

2.9. Determination of infarct size

The brains were sectioned into 2-μm slices, stained with 2,3,5-triphenyltetrazolium chloride (TTC, 0.2%) at 37 °C for 30 min and fixed in 10% formalin. The brains that showed clot formation and/or subarachnoid hemorrhage were excluded from analysis. The tissue slices were subsequently photographed, and the infarct size and relative infarct ratio were determined as previously described (Zhang et al., 2017). DAKP1 was detected by immunohistochemistry. The analysis was conducted by a histologist blinded to treatment conditions.

2.10. Neurological deficit assessment

The neurological status was assessed 24 h after reperfusion by a neurologic deficit score as described previously (Zhang et al., 2017). The deficit scores were defined as: 0 = no observable deficits; 1 = difficult to fully extend the contralateral forelimb; 2 = unable to extend the contralateral forelimb; 3 = mild circling to the contralateral side; 4 = severe circling to the contralateral side; 5 = falling to the contralateral side. Animals were evaluated and scored by a scientist blinded to treatment conditions.

2.11. TUNEL assay

Apoptosis was assessed by TUNEL staining using the ApopTag Kit-S7100 from Chemicon (Temecula, CA, USA) following manufacturer's instructions. Cells were photographed with a CoolSNAP photometric camera. TUNEL positive cell nuclei were counted under a Nikon ECLIPSE Ti fluorescence microscope (×200 magnification). The rate of apoptosis (%) was calculated as the percentage of TUNEL positive cell nuclei in 10 random fields for each sample.

2.12. Statistical analysis

Data are presented as means ± S.E.M. from at least three independent experiments. Statistical analysis was performed using GraphPad Prism 5.01 software (GraphPad Software, La Jolla, CA, USA). Results from two different groups were compared by Student's *t*-test. Differences with a P value $< .05$ were deemed statistically significant.

3. Results

3.1. AK038897 is upregulated and miR-26a is downregulated following neuronal I/R in vitro and in vivo

Using StarBase (http://starbase.sysu.edu.cn/mirMrna.php) and TargetScan (http://www.targetscan.org), we identified putative miR-26a-5p binding sites in AK038897 as well as in the 3′-UTR of DAPK1, a central mediator of ischemic neuronal death (Shamloo et al., 2005; Tu et al., 2010). Thus, we proposed that miR-26a-5p may directly regulate DAPK1 expression, and AK038897 may indirectly control DAPK1 by competing for miR-26a-5p binding. As such, the AK038897/miR-26a-5p/DAPK1 axis may regulate ischemic neuronal death. To evaluate this hypothesis, we determined the expression of AK038897 and miR-26a-5p in *in vitro* and *in vivo* models of cerebral I/R. Mice subjected to MCAO/R (1 h/24 h) exhibited substantial neurologic dysfunction and severe cerebral infarction (Fig. 1A–C). Compared with the corresponding control, higher AK038897 and lower miR-26a-5p levels were detected following I/R treatment *in vivo* (Fig. 1D, E). The western blot analysis revealed increased C-caspase-3, C-PARP and Bax along with decreased Bcl-2 levels in the brain (Fig. 1F), confirming brain cell damage by apoptosis. In addition, N2a cells subjected to OGD/R (3 h/24 h), an increasing AK038897 and a decreasing miR-26a-5p were also detected *in vitro* (Fig. 1G, H). The treated-cells suffered significant apoptosis as indicated by TUNEL staining and western blot analysis of apoptosis-related proteins (Fig. 1I–K).

3.2. AK038897 binds to miR-26a-5p and regulates miR-26a-5p expression

To test the relationship between AK038897 and miR-26a-5p, we constructed luciferase reporter systems carrying the wild type AK038897 (AK038897-WT) or a mutant AK038897 with mutations at

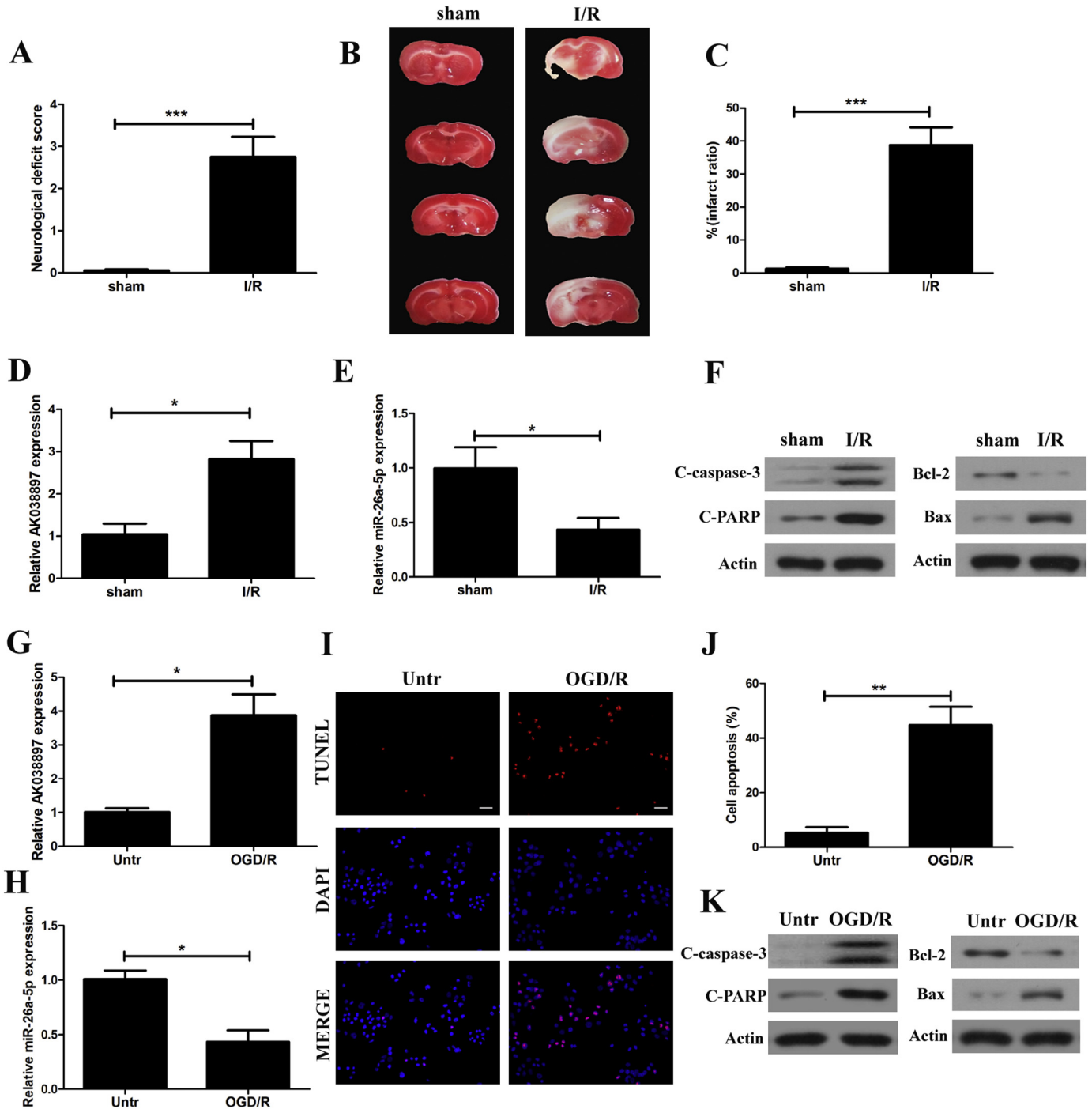

Fig. 1. AK038897 is upregulated and miR-26a is downregulated in *in vitro* and *in vivo* models of ischemic stroke. (A–F) Male C57BL/6J mice were subjected to MCAO/R (1 h/24 h) or sham operation. (A) Neurological deficit scores. (B) Images of brain sections with TTC staining. (C) Cerebral infarct ratio. (D, E) Cerebral AK038897 (D) and miR-26a-5p (E) levels by qRT-PCR. (F) Cerebral C-caspase-3, C-PARP, Bcl-2 and Bax levels by western blot analysis. n = 6 per group, *P < .05, ***P < .001. (G–K) N2a cells were subjected to OGD/R (3 h/24 h). Untreated cells (Untr) were included as control. (G, H) AK038897 (G) and miR-26a-5p (H) levels by qRT-PCR. (I, J) Cell apoptosis was measured by TUNEL staining. Representative cell images (I, Scale bar = 25 μm) and quantified cell apoptosis percentage (J) are shown. (K) C-caspase-3, C-PARP, Bcl-2 and Bax levels by western blot analysis. n = 3, *P < .05, **P < .01.

the putative miR-26a-5p binding site (AK038897-MUT) (Fig. 2A). We found that cotransfection with miR-26a-5p mimic decreased while co-transfection with miR-26a-5p inhibitor increased the luciferase activity in AK038897-WT but not in AK038897-MUT-transfected N2a cells (Fig. 2B, C), suggesting that miR-26a-5p binds to AK038897 at the predicted binding site. The RNA immunoprecipitation assay results confirmed physical association between AK038897 and miR-26a-5p in N2a cells (Fig. 2D). Furthermore, AK038897 overexpression in N2a cells led to reduced miR-26a-5p expression while expression of si-AK038897 resulted in the opposite effects (Fig. 2E, F). Taken together, these data supported that AK038897 can downregulate miR-26a-5p activity *via* two mechanisms: 1) Acting as a ceRNA by competing for binding to miR-26a-5p and 2) Downregulating miR-26a-5p expression.

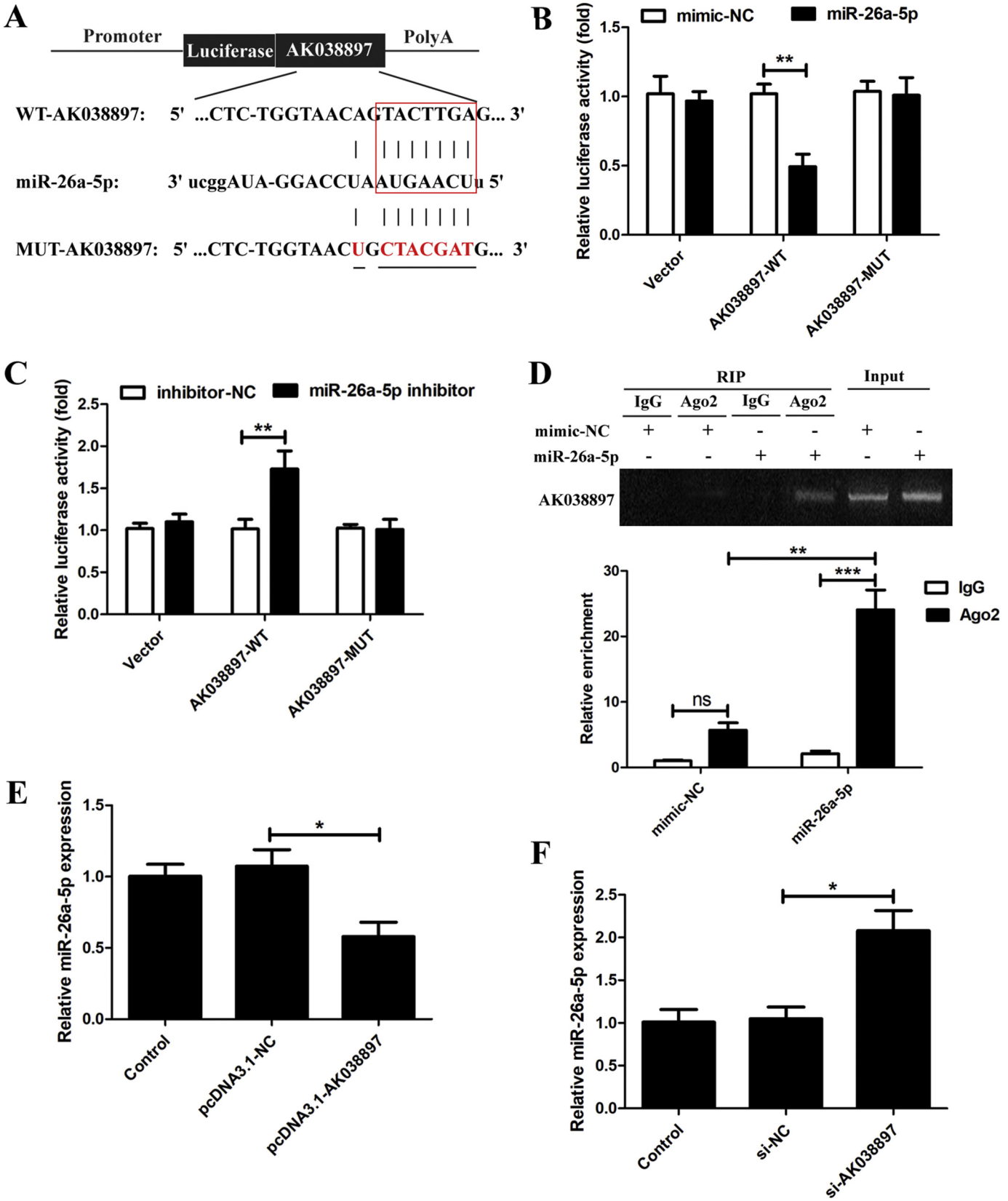

Fig. 2. AK038897 binds to miR-26a-5p and regulates miR-26a-5p expression. (A) The wild type AK038897 (AK038897-WT) and a mutant AK038897 with mutations at the predicted miR-26a binding site (AK038897-MUT). (B, C) The luciferase reporter vector carrying AK038897-WT or AK038897-MUT or the empty vector was cotransfected with miR-26a-5p mimic or mimic-NC (B) or miR-26a-5p inhibitor or inhibitor-NC (C) as indicated into N2a cells. The relative luciferase activity was detected 48 h after transfection. (D) N2a cells were transfected with miR-26a-5p mimic or mimic-NC for 48 h. The association between AK038897 and miR-26a-5p was assessed by RNA immunoprecipitation assay. (E, F) N2a cells were transfected with pcDNA3.1-AK038897 or pcDNA3.1-NC (E) or si-AK038897 or si-NC (F) for 48 h. Untransfected cells were included as control (Control). The expression of miR-26a-5p was determined by qRT-PCR. n = 3, *P < .05, **P < .01, ***P < .001, ns = not significant.

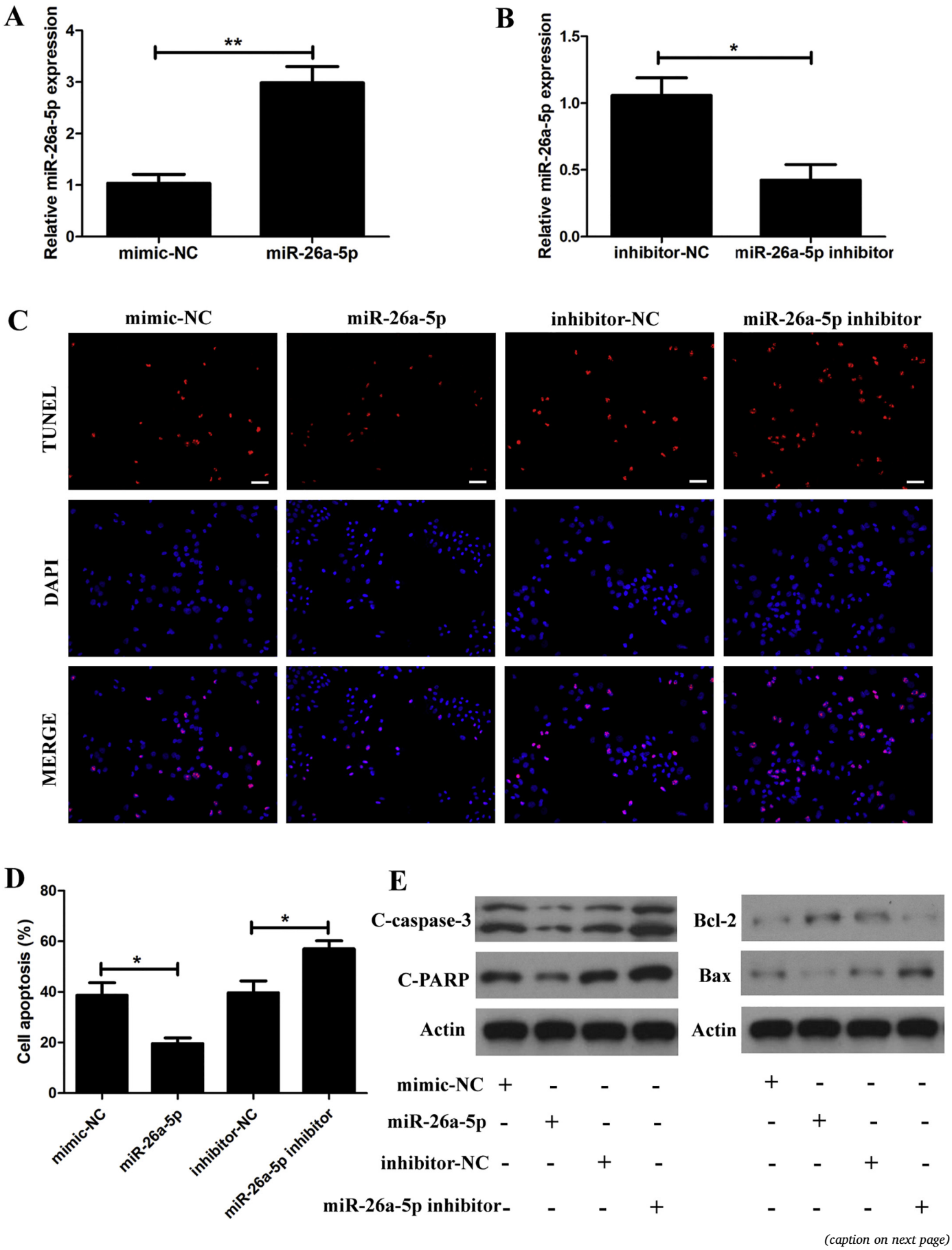

(caption on next page)

Fig. 3. miR-26a-5p attenuates OGD/R-induced neuronal apoptosis. (A, B) N2a cells were transfected with miR-26a-5p mimic or mimic-NC (A) or miR-26a-5p inhibitor or inhibitor-NC (B) for 48 h. The miR-26a-5p levels were determined by qRT-PCR. (C–E) N2a cells transfected with miR-26a-5p mimic, mimic-NC, miR-26a-5p inhibitor or inhibitor-NC for 48 h were exposed to OGD/R (3 h/24 h). (C, D) Cell apoptosis was measured by TUNEL staining. Representative cell images (C, Scale bar = 25 μm) and quantified cell apoptosis percentage (D) are shown. (E) C-caspase-3, C-PARP, Bcl-2 and Bax levels by western blot analysis. n = 3, *P < .05, **P < .01.

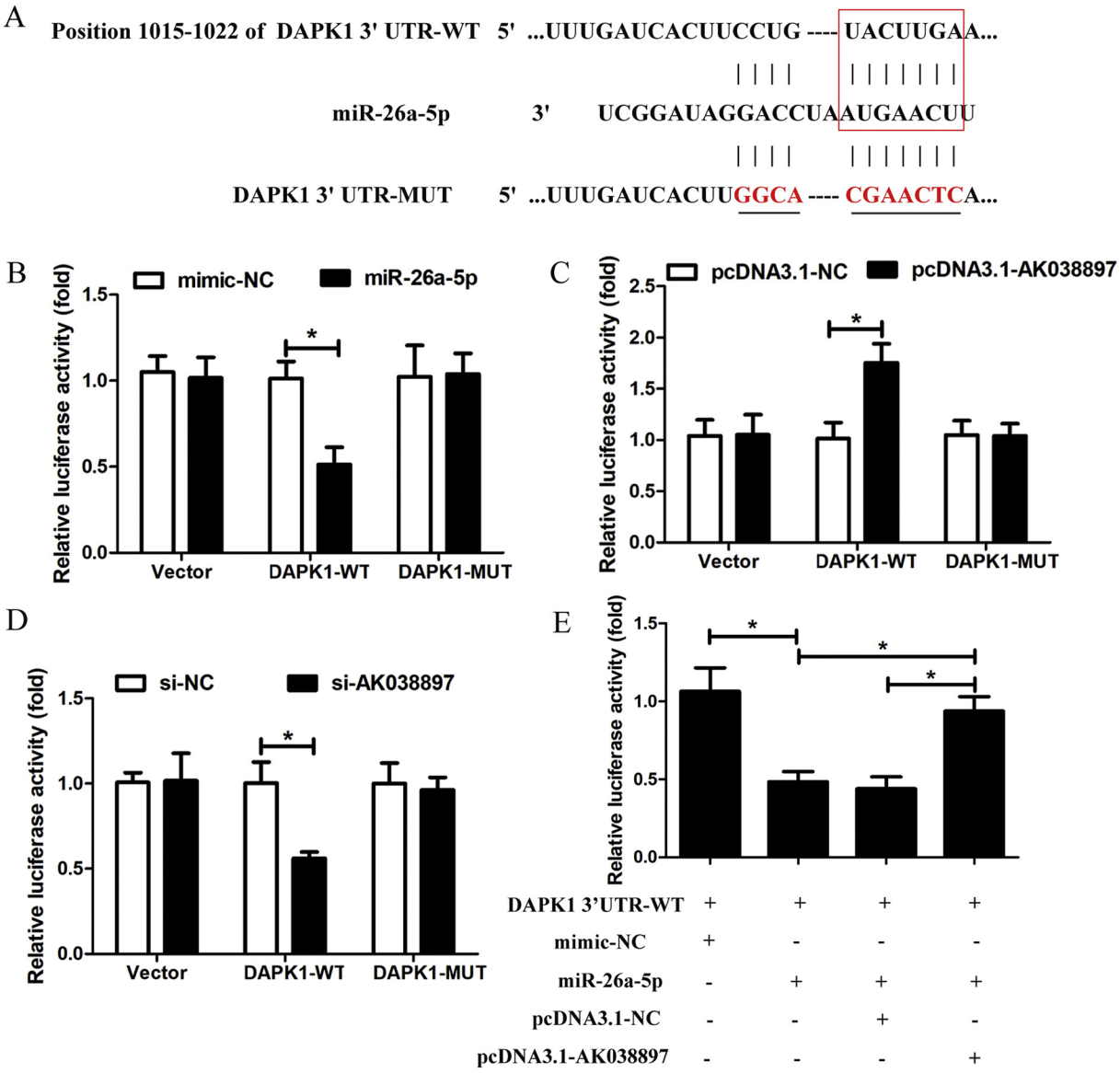

Fig. 4. AK038897 competes with 3′-UTR of DAPK1 mRNA for binding to miR-26a-5p. (A) The wild type 3′-UTR of DAPK1 (DAPK1 3′-UTR-WT) and a mutant 3′-UTR of DAPK1 with mutations at the predicted miR-26a-5p binding site (DAPK1 3′-UTR-MUT). (B–D) The luciferase reporter vector carrying DAPK1 3′-UTR-WT or DAPK1 3′-UTR-MUT or the empty vector was cotransfected with miR-26a-5p mimic or mimic-NC (B), pcDNA3.1-AK038897 or pcDNA3.1-NC (C) or si-AK038897 or si-NC (D) as indicated into N2a cells. The relative luciferase activity was detected 48 h after transfection. (E) The luciferase reporter vector carrying DAPK1 3′-UTR-WT was cotransfected with miR-26a-5p mimic, mimic-NC, pcDNA3.1-AK038897 and pcDNA3.1-NC, alone or in combination as indicated into N2a cells. The relative luciferase activity was determined 48 h after transfection. n = 3, *P < .05.

3.3. MiR-26a-5p attenuates OGD/R-induced neuronal apoptosis

To test the function of miR-26a-5p in neuronal I/R injury, we transfected N2a cells with miR-26a-5p mimic and miR-26a-5p inhibitor, respectively. The miR-26a-5p overexpression and knockdown were confirmed by qRT-PCR (Fig. 3A, B). Following OGD/R (3 h/24 h), N2a cells overexpressing miR-26a-5p exhibited reduced apoptosis and those with miR-26a-5p knockdown showed increased apoptotic cell death compared with the corresponding control as indicated by TUNEL staining (Fig. 3C, D). Western blot analysis of the apoptosis-related proteins C-caspase-3, C-PARP, Bcl-2 and Bax confirmed the effects of miR-26a-5p overexpression or knockdown on OGD/R-induced cell apoptosis (Fig. 3E).

3.4. AK038897 acts as a ceRNA for miR-26a-5p to target DAPK1

To find out whether DAPK1 is a *bona fide* target of miR-26a-5p, we constructed luciferase reporter systems carrying The wild type 3′-UTR of DAPK1 (DAPK1 3′-UTR-WT) or a mutant 3′-UTR of DAPK1 with mutations at the predicted miR-26a-5p binding site (DAPK1 3′-UTR-

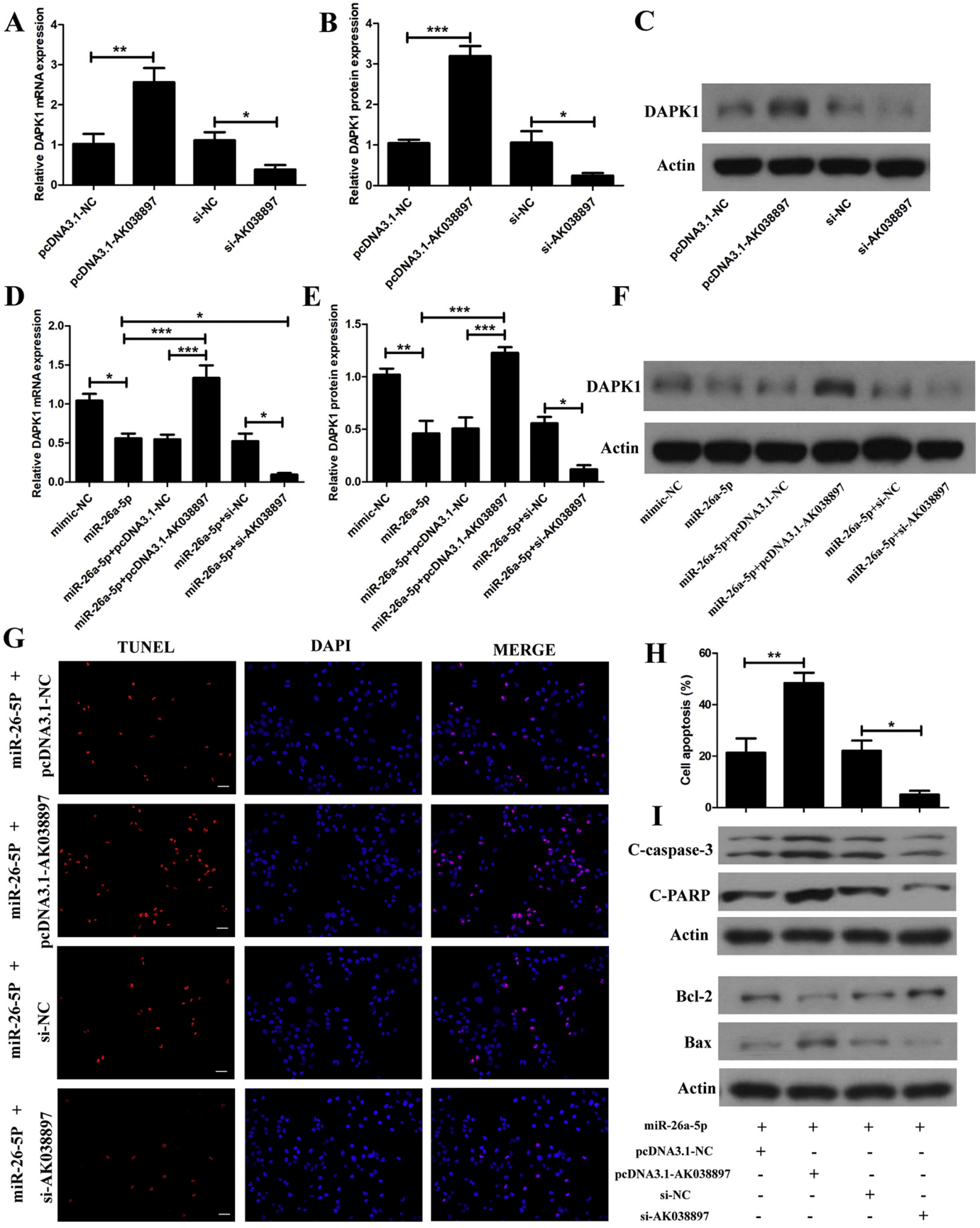

(caption on next page)

Fig. 5. AK038897 antagonizes the inhibitory effects of miR-26a-5p on DAPK1 to regulate OGD/R-induced neuronal apoptosis. (A–C) The relative DAPK1 mRNA (A) and protein (B, C) levels in N2a cells stably transfected with pcDNA3.1-AK038897, pcDNA3.1-NC, si-AK038897 or si-NC detected by qRT-PCR and western blot analysis, respectively. (D–F) N2a cells stably transfected with pcDNA3.1-AK038897, pcDNA3.1-NC, si-AK038897 or si-NC were transiently transfected with miR-26a-5p mimic for 48 h. Untransfected N2a cells were transiently transfected with miR-26a-5p mimic or mimic-NC for 48 h. The relative DAPK1 mRNA (D) and protein (E, F) levels were determined by qRT-PCR and western blot analysis, respectively. (G–I) N2a cells stably transfected with pcDNA3.1-AK038897, pcDNA3.1-NC, si-AK038897 or si-NC were transiently transfected with miR-26a-5p mimic for 48 h. The cells were subsequently exposed to OGD/R (3 h/24 h). (G, H) Cell apoptosis was measured by TUNEL staining. Representative cell images (G, Scale bar = 25 μm) and quantified cell apoptosis percentage (H) are shown. (I) C-caspase-3, C-PARP, Bcl-2 and Bax levels by western blot analysis. n = 3, *P < .05, **P < .01, ***P < .001.

MUT) (Fig. 4A). The results showed that cotransfection with miR-26a-5p mimic decreased the luciferase activity in DAPK1 3′-UTR-WT but not in DAPK1 3′-UTR-MUT-transfected N2a cells (Fig. 4B), indicating that miR-26a-5p directly targets DAPK1 by binding to DAPK1 3′-UTR at the predicted binding site. In contrast, AK038897 overexpression increased while AK038897 knockdown decreased the DAPK1 3′-UTR-dependent luciferase reporter expression (Fig. 4C, D). In addition, AK038897 overexpression reversed the inhibitory effects of miR-26a-5p mimics on DAPK1 3′-UTR-dependent luciferase reporter expression (Fig. 4E). These data, taken together with the fact that we have detected direct binding between AK038897 and miR-26a-5p, indicated that AK038897 regulates DAPK1 by acting as a ceRNA for miR-26a-5p.

3.5. AK038897 antagonizes the inhibitory effects of miR-26a-5p mimics on DAPK1 to regulate OGD/R-induced neuronal apoptosis

To test the function of AK038897 in neuronal I/R injury, we prepared N2a cells stably transfected with pcDNA3.1-AK038897, pcDNA3.1-NC, si-AK038897 or si-NC. In alignment with the effects of AK038897 on DAPK1 3′-UTR-dependent luciferase reporter expression, AK038897 overexpression increased while AK038897 knockdown decreased DAPK1 expression in N2a cells as indicated by qRT-PCR and western blot analysis (Fig. 5A–C). Moreover, AK038897 overexpression antagonized while AK038897 knockdown enhanced the inhibitory effects of miR-26a-5p mimics on DAPK1 (Fig. 5D–F). Consequently, AK038897 overexpression restored OGD/R-induced N2a cell apoptosis inhibited by miR-26a-5p mimics while AK038897 knockdown had the opposite effects as revealed by TUNEL staining and western blot analysis of apoptosis-related proteins (Fig. 5G–I).

3.6. AK038897 knockdown downregulates DAPK1 and protects against cerebral I/R injury in vivo

Finally, we tested the function of AK038897 in cerebral I/R injury *in vivo*. Compared with sham control, mouse brains exposed to MCAO/R (1 h/24 h) exhibited increased AK038897 along with decreased miR-26a-5p and increased DAPK1 (Fig. 6A–F). In alignment with the AK038897/miR-26a-5p/DAPK1 signaling cascade detected in N2a cells *in vitro*, AK038897 knockdown in mouse brain by si-AK038897 injection resulted in increased miR-26a-5p and decreased DAPK1 expression (Fig. 6A–F). Consequently, AK038897-silenced mice exhibited reduced cerebral infarction (Fig. 6G, H), neurological deficits (Fig. 6I) and brain cell apoptosis (Fig. 6J–L) following MCAO/R compared with control.

4. Discussion

miRNA is conventionally considered an “initiator” and unilateral regulator of mRNA expression. miRNAs bind to MREs (miRNA response elements) in the 3′-UTR of the target mRNA, resulting in downregulation of the target gene mediated by Argonaute (Ago) proteins (Bartel, 2009; Thomas et al., 2010). However, research advances over the past decade have revealed that pseudogenes, lncRNAs and circular RNAs (circRNAs) can act as ceRNAs by binding to shared MREs, lowering the levels of miRNAs available for the target mRNA (Ebert and Sharp, 2010; Sen et al., 2014). Accordingly, the role of miRNAs in regulating gene expression has since been modified from that of an “initiator” to a “mediator”, with the regulation pattern revised from miRNAs → mRNAs to ceRNAs → miRNAs → mRNAs (Ala et al., 2013; Liu et al., 2017). By regulating miRNAs and the target mRNA translation, ceRNAs have been implicated in many biological processes and pathological conditions such as cancer and pulmonary arterial hypertension (Cesana et al., 2011; Liu et al., 2017; Ma et al., 2014). In particular, studies in recent years have highlighted the role of lncRNAs functioning as ceRNAs in the pathogenesis of ischemic stroke. For instance, lncRNA MEG3 regulates ischemic neuronal death *in vitro* and *in vivo* by acting as a ceRNA to target the miR-21/PDCD4 signaling pathway (Yan et al., 2017). In addition, lncRNA GAS5 regulates ischemic stroke as a ceRNA for miR-137 to modulate Notch1 (Chen et al., 2018). These findings underscore the ceRNAs → miRNAs → regulatory axis as a potential target for treatment of ischemic stroke.

In this work, we identified lncRNA AK038897 as a regulator of ischemic stroke by acting as a ceRNA for miR-26a-5p to target DAPK1. Similar to previous findings (Wu et al., 2017), we detected markedly increased AK038897 levels in mouse brains subjected to transient focal ischemia as well as in neuronal cells exposed to OGD/R. In addition, AK038897 knockdown protected against cerebral I/R-induced brain damage and neurological dysfunction *in vivo*. With bioinformatics, we identified shared putative miR-26a-5p binding sites in AK038897 as well as in the 3′-UTR of DAPK1, a central mediator of ischemic neuronal death (Shamloo et al., 2005; Tu et al., 2010). MiR-26a-5p has been shown to promote osteogenic differentiation (Li et al., 2016), regulate tumor metastasis (Chang et al., 2017; Guo et al., 2016; Song et al., 2018) and suppress the autophagic pathway in cardiac fibroblasts (Zheng et al., 2018). However, the function of miR-26a-5p in ischemic stroke is not clear. In this study, miR-26a-5p expression exhibited changes opposite to those of AK038897 in response to I/R *in vitro* and *in vivo*. The luciferase reporter assay results confirmed that miR-26a-5p directly targets DAPK1. To the best of our knowledge, this is the first report on DAPK1 as a target of miR-26a-5p. Further mechanistic studies revealed that AK038897 downregulates miR-26a-5p expression and acts as a ceRNA for miR-26a-5p to regulate DAPK1. As a result, AK038897 aggravates neuronal I/R injury *in vitro* and *in vivo*. Thus, we identified a novel AK038897 → miR-26a-5p → DAPK1 signaling axis as a key regulatory mechanism in ischemic stroke. In addition, miR-26a-5p was also reported to inhibit endothelial apoptosis and inflammatory response *via* targeting TLR4 mRNA and suppressing NF-κB pathway (Feng et al., 2018; Zhong et al., 2018), which might be also involved in si-AK038897's protective effects. The AK038897 long non-coding RNA may also have additional binding sites for other miRNA targets, which are not described in this paper. Thus, more and further mechanisms for the effects of AK038897 should be explored in the future.

5. Conclusions

In summary, our results indicated that lncRNA AK038897 targets DAPK1 by acting as a ceRNA for miR-26a-5p to regulate ischemic stroke. The pharmaceutical intervention of the AK038897/miR-26a-5p/DAPK1 signaling cascade may provide therapeutic benefits for ischemic stroke.

Supplementary data to this article can be found online at https://doi.org/10.1016/j.expneurol.2019.01.009.

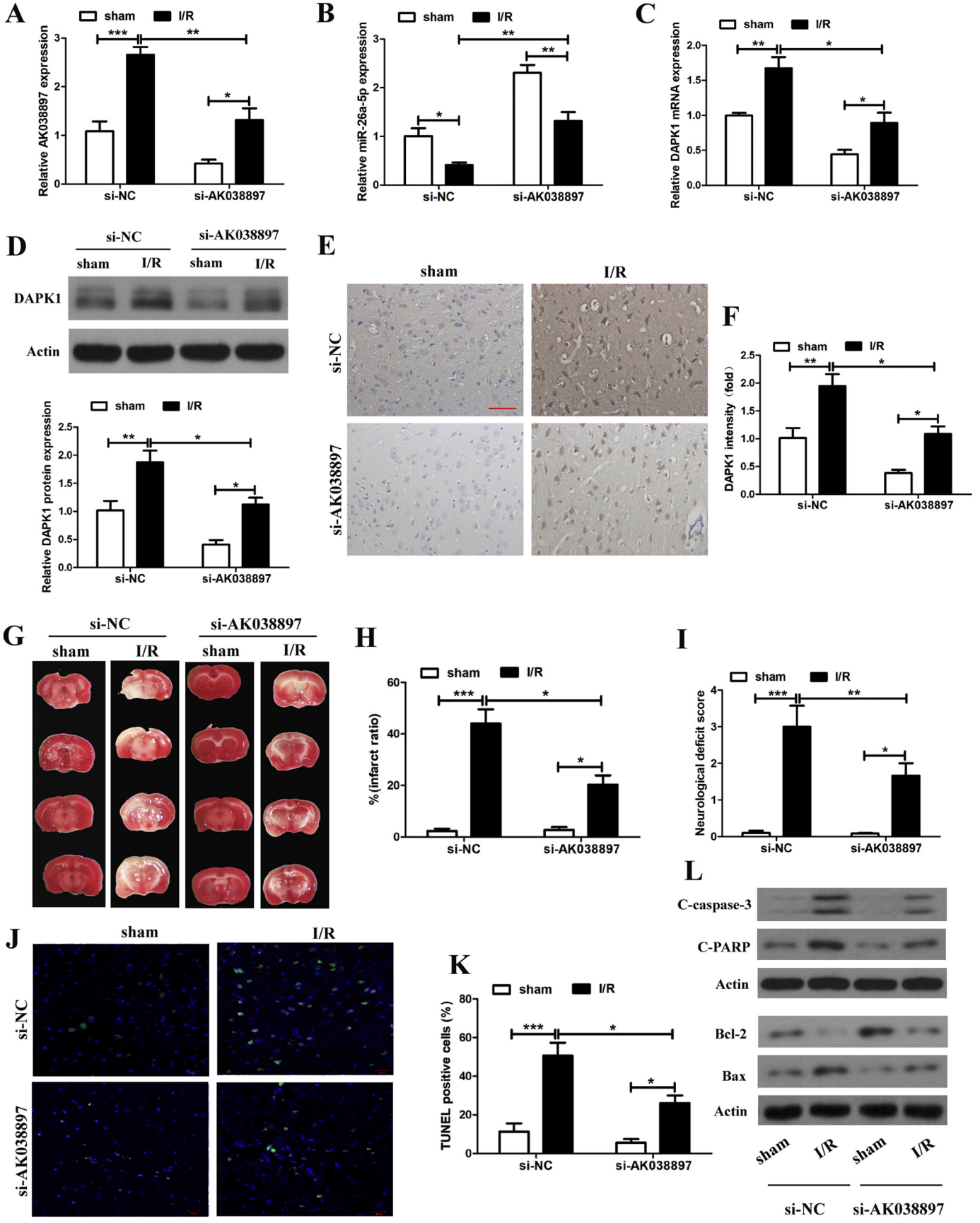

(caption on next page)

Fig. 6. AK038897 knockdown protects against cerebral I/R injury *in vivo*. (A–F) si-AK038897 or si-NC was injected into the lateral ventricle of mice. At 24 h after the injection, the mice were subjected to MCAO/R (1 h/24 h) or sham operation, and the brains were isolated for analysis. (A–C) Cerebral AK038897 (A), miR-26a-5p (B) and DAPK1 (C) mRNA levels by qRT-PCR. (D–F) DAPK1 protein levels by western blot (D) or immunohistochemistry (E, F) (Scale bar = 50 μm). n = 6 per group, *P < .05, **P < .01. (G) Images of brain sections with TTC staining. (H) Cerebral infarct ratio. (I) Neurological deficit score. (J, K) Cell apoptosis in cerebral cortex was measured by TUNEL staining. Representative cell images (J, Scale bar = 20 μm) and quantified cell apoptosis percentage (K) are shown. n = 6 per group, *P < .05, ***P < .001. (L) C-caspase-3, C-PARP, Bcl-2 and Bax levels by western blot analysis.

Acknowledgments

This project was supported by The National Natural Science Foundation of China (No. 81560319, No. 81760349), Natural Science Foundation of Yunnan Province, China (No.2016FB130), and Science Foundation of Health and Family Planning Committee of Yunnan Province (No. 2016NS066, No. 2018NS0135).

References

Ala, U., Karreth, F.A., Bosia, C., Pagnani, A., Taulli, R., Leopold, V., Tay, Y., Provero, P., Zecchina, R., Pandolfi, P.P., 2013. Integrated transcriptional and competitive endogenous RNA networks are cross-regulated in permissive molecular environments. Proc. Natl. Acad. Sci. U. S. A. 110, 7154–7159.

Bartel, D.P., 2009. MicroRNAs: target recognition and regulatory functions. Cell 136, 215–233.

Bialik, S., Kimchi, A., 2006. The death-associated protein kinases: structure, function, and beyond. Annu. Rev. Biochem. 75, 189–210.

Blakeley, J.O., Llinas, R.H., 2007. Thrombolytic therapy for acute ischemic stroke. J. Neurol. Sci. 261, 55–62.

Cesana, M., Cacchiarelli, D., Legnini, I., Santini, T., Sthandier, O., Chinappi, M., Tramontano, A., Bozzoni, I., 2011. A long noncoding RNA controls muscle differentiation by functioning as a competing endogenous RNA. Cell 147, 358–369.

Chang, L., Li, K., Guo, T., 2017. miR-26a-5p suppresses tumor metastasis by regulating EMT and is associated with prognosis in HCC. Clin. Transl. Oncol. 19, 695–703.

Chen, F., Zhang, L., Wang, E., Zhang, C., Li, X., 2018. LncRNA GAS5 regulates ischemic stroke as a competing endogenous RNA for miR-137 to regulate the Notch1 signaling pathway. Biochem. Biophys. Res. Commun. 496, 184–190.

Cohen, O., Inbal, B., Kissil, J.L., Raveh, T., Berissi, H., Spivak-Kroizaman, T., Feinstein, E., Kimchi, A., 1999. DAP-kinase participates in TNF-alpha- and Fas-induced apoptosis and its function requires the death domain. J. Cell Biol. 146, 141–148.

Deiss, L.P., Feinstein, E., Berissi, H., Cohen, O., Kimchi, A., 1995. Identification of a novel serine/threonine kinase and a novel 15-kD protein as potential mediators of the gamma interferon-induced cell death. Genes Dev. 9, 15–30.

Dharap, A., Bowen, K., Place, R., Li, L.C., Vemuganti, R., 2009. Transient focal ischemia induces extensive temporal changes in rat cerebral microRNAome. J. Cereb. Blood Flow Metab. 29, 675–687.

Dharap, A., Nakka, V.P., Vemuganti, R., 2012. Effect of focal ischemia on long noncoding RNAs. Stroke 43, 2800–2802.

Ebert, M.S., Sharp, P.A., 2010. MicroRNA sponges: progress and possibilities. RNA 16, 2043–2050.

Feng, M., Xu, D., Wang, L., 2018. miR-26a inhibits atherosclerosis progression by targeting TRPC3. Cell Biosci. 8, 4.

Guo, K., Zheng, S., Xu, Y., Xu, A., Chen, B., Wen, Y., 2016. Loss of miR-26a-5p promotes proliferation, migration, and invasion in prostate cancer through negatively regulating SERBP1. Tumour Biol. 37, 12843–12854.

Guo, D., Ma, J., Yan, L., Li, T., Li, Z., Han, X., Shui, S., 2017. Down-regulation of Lncrna MALAT1 attenuates neuronal cell death through suppressing Beclin1-dependent autophagy by regulating Mir-30a in cerebral ischemic stroke. Cell. Physiol. Biochem. 43, 182–194.

Li, S., Hu, C., Li, J., Liu, L., Jing, W., Tang, W., Tian, W., Long, J., 2016. Effect of miR-26a-5p on the Wnt/Ca(2+) pathway and osteogenic differentiation of mouse adipose-derived mesenchymal stem cells. Calcif. Tissue Int. 99, 174–186.

Li, G., Morris-Blanco, K.C., Lopez, M.S., Yang, T., Zhao, H., Vemuganti, R., Luo, Y., 2018. Impact of microRNAs on ischemic stroke: from pre- to post-disease. Prog. Neurobiol. 163-164, 59–78.

Liu, Y., Wang, Z., Huang, D., Wu, C., Li, H., Zhang, X., Meng, B., Li, Z., Zhu, T., Yang, S., Sun, W., 2017. LMO2 promotes tumor cell invasion and metastasis in basal-type breast cancer by altering actin cytoskeleton remodeling. Oncotarget 8, 9513–9524.

Ma, K., Zhao, Q., Li, S., 2014. Competing endogenous RNA network in pulmonary arterial hypertension. Int. J. Cardiol. 172, e527–e528.

Martinez, B., Peplow, P.V., 2017. Immunomodulators and microRNAs as neurorestorative therapy for ischemic stroke. Neural Regen. Res. 12, 865–874.

Musuka, T.D., Wilton, S.B., Traboulsi, M., Hill, M.D., 2015. Diagnosis and management of acute ischemic stroke: speed is critical. CMAJ 187, 887–893.

Nour, M., Scalzo, F., Liebeskind, D.S., 2013. Ischemia-reperfusion injury in stroke. Interv. Neurol. 1, 185–199.

Pelled, D., Raveh, T., Riebeling, C., Fridkin, M., Berissi, H., Futerman, A.H., Kimchi, A., 2002. Death-associated protein (DAP) kinase plays a central role in ceramide-induced apoptosis in cultured hippocampal neurons. J. Biol. Chem. 277, 1957–1961.

Sen, R., Ghosal, S., Das, S., Balti, S., Chakrabarti, J., 2014. Competing endogenous RNA: the key to posttranscriptional regulation. ScientificWorldJournal 2014, 896206.

Shamloo, M., Soriano, L., Wieloch, T., Nikolich, K., Urfer, R., Oksenberg, D., 2005. Death-associated protein kinase is activated by dephosphorylation in response to cerebral ischemia. J. Biol. Chem. 280, 42290–42299.

Song, Q., Liu, B., Li, X., Zhang, Q., Cao, L., Xu, M., Meng, Z., Wu, X., Xu, K., 2018. MiR-26a-5p potentiates metastasis of human lung cancer cells by regulating ITGbeta8-JAK2/STAT3 axis. Biochem. Biophys. Res. Commun. 501, 494–500.

Thomas, M., Lieberman, J., Lal, A., 2010. Desperately seeking microRNA targets. Nat. Struct. Mol. Biol. 17, 1169–1174.

Tu, W., Xu, X., Peng, L., Zhong, X., Zhang, W., Soundarapandian, M.M., Balel, C., Wang, M., Jia, N., Zhang, W., Lew, F., Chan, S.L., Chen, Y., Lu, Y., 2010. DAPK1 interaction with NMDA receptor NR2B subunits mediates brain damage in stroke. Cell 140, 222–234.

Wang, Z., Qu, L., Deng, B., Sun, X., Wu, S., Liao, J., Fan, J., Peng, Z., 2016. STYK1 promotes epithelial-mesenchymal transition and tumor metastasis in human hepatocellular carcinoma through MEK/ERK and PI3K/AKT signaling. Sci. Rep. 6, 33205.

Wu, Z., Wu, P., Zuo, X., Yu, N., Qin, Y., Xu, Q., He, S., Cen, B., Liao, W., Ji, A., 2017. LncRNA-N1LR enhances neuroprotection against Ischemic Stroke probably by Inhibiting p53 phosphorylation. Mol. Neurobiol. 54, 7670–7685.

Yan, H., Yuan, J., Gao, L., Rao, J., Hu, J., 2016. Long noncoding RNA MEG3 activation of p53 mediates ischemic neuronal death in stroke. Neuroscience 337, 191–199.

Yan, H., Rao, J., Yuan, J., Gao, L., Huang, W., Zhao, L., Ren, J., 2017. Long non-coding RNA MEG3 functions as a competing endogenous RNA to regulate ischemic neuronal death by targeting miR-21/PDCD4 signaling pathway. Cell Death Dis. 8, 3211.

Zhang, W., Wei, R., Zhang, L., Tan, Y., Qian, C., 2017. Sirtuin 6 protects the brain from cerebral ischemia/reperfusion injury through NRF2 activation. Neuroscience 366, 95–104.

Zheng, L., Lin, S., Lv, C., 2018. MiR-26a-5p regulates cardiac fibroblasts collagen expression by targeting ULK1. Sci. Rep. 8, 2104.

Zhong, X., Zhang, L., Li, Y., Li, P., Li, J., Cheng, G., 2018. Kaempferol alleviates ox-LDL-induced apoptosis by up-regulation of miR-26a-5p via inhibiting TLR4/NF-kappaB pathway in human endothelial cells. Biomed. Pharmacother. 108, 1783–1789.